CSIRO PUBLISHING

Australian Journal of Physics

Volume 50, 1997

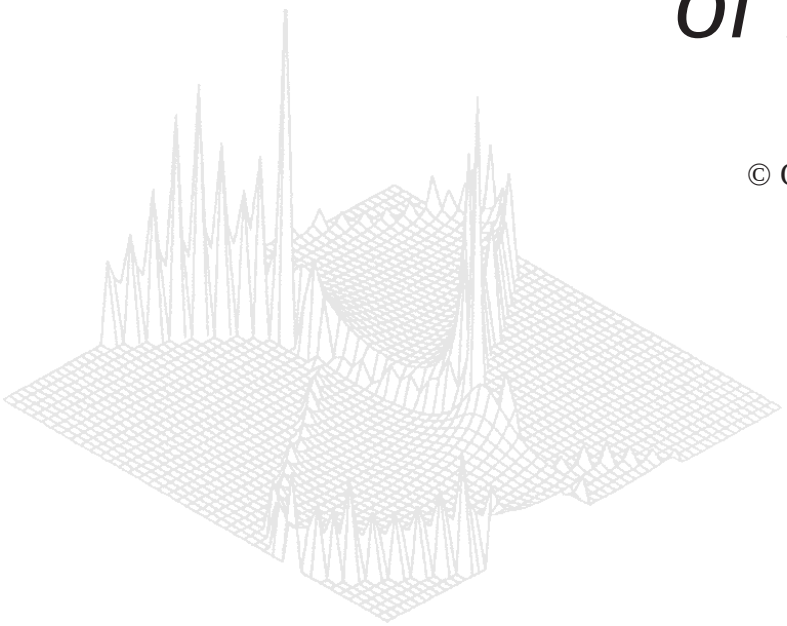

A journal for the publication of
original research in all branches of physics

www.publish.csiro.au/journals/ajp

All enquiries and manuscripts should be directed to
Australian Journal of Physics
CSIRO PUBLISHING
PO Box 1139 (150 Oxford St)
Collingwood Telephone: 61 3 9662 7626
Vic. 3066 Facsimile: 61 3 9662 7611
Australia Email: peter.robertson@publish.csiro.au

Published by **CSIRO** PUBLISHING
for CSIRO Australia and
the Australian Academy of Science

Aust. J. Phys., 1998, **51**, 131–42

Magnetic Transition and Spin Correlation in Mn Oxides at Low Temperatures

Jie Jiang

Department of Physics, National Laboratory of Solid State Microstructures, Nanjing University, Nanjing 210 008, P.R. China.

Abstract

We study the magnetic transition and spin correlation in Mn oxides at low temperatures. The results indicate that there are antiferromagnetic (AF), spiral (SP), ferromagnetic (FM) and canted (CN) states when $T \to 0$. With temperature increasing, a paramagnetic (PM) state appears. The spin–spin correlation function is also obtained.

1. Introduction

The perovskite Mn oxides $Re_{1-x}A_xMnO_3$ (here Re is a rare earth such as La and A is a divalent element such as Sr or Ca) have prompted considerable theoretical and experimental interest because of a large negative magnetoresistance near room temperature (Ju *et al*. 1994; von Helmolt *et al*. 1993, 1994). In the interesting doping range $0{\cdot}2 < x < 0{\cdot}5$, $Re_{1-x}A_xMnO_3$ is a ferromagnetic metal at low temperatures. In order to explain this phenomenon, a double exchange model was proposed (Zener 1951; Anderson and Hasegawa 1955). The model involves spin coupling between Mn^{+3} and Mn^{+4} next-nearest-neighbour ions with the conduction electrons mediating the interaction. Recently, it has been pointed out that in order to understand the extraordinary magnetoresistance phenomena in these materials the electron–phonon interaction should be included (Hwang *et al*. 1995; Ibarra *et al*. 1995; Mills *et al*. 1995, 1996). In spite of this, the rough correspondence between the optical and magnetic measurements of the electron stress-energy tensor suggests that the double exchange model provides a good representation of the physics at low temperatures (Mills *et al*. 1995).

In the case of low temperature, the double exchange model alone is reasonable (Mills *et al*. 1995). In this case, a phase diagram has been given by Inoue and Maekawa (1995). However, they only considered AF, SP, FM and CN states. A PM state, which may naturally appear with T increasing, is not considered. Moreover, they treated the model Hamiltonian in a conventional mean field level which cannot give the spin–spin correlation function. Thus, a further study is needed. In treating the strongly correlated system, the Schwinger boson method is useful as it gives a good approximation to the ground state (Yoshioka 1989; Auerbach and Aovas 1988). At finite temperatures its results are consistent with those by computer simulation (Yoshioka 1989). In this paper,

 10.1071/PH96108 0004-9506/98/010131$05.00

we use the Schwinger boson method to treat the model Hamiltonian to obtain a detailed phase diagram in the $x - k_B T$ plane at low temperatures and a spin–spin correlation function.

2. Model Hamiltonian and Treatment Method

We treat t_{2g} and e_g electrons of Mn ions in $Re_{1-x}A_xMnO_3$ as local spins of $S = \frac{3}{2}$ and itinerant electrons of $S = \frac{1}{2}$, respectively. The Hamiltonian describing these materials can be expressed as (Inoue and Maekawa 1995)

$$H = -t \sum_{\langle ij \rangle \sigma} a^{\dagger}_{i\sigma} a_{j\sigma} + \sum_{i\sigma} \epsilon_0 a^{\dagger}_{i\sigma} a_{i\sigma} + \frac{U}{2} \sum_{i\sigma} n_{i\sigma} n_{i\bar{\sigma}}$$

$$+ J \sum_{\langle ij \rangle} \mathbf{S}_i \,.\, \mathbf{S}_j - \frac{K}{2} \sum_i \mathbf{S}_i \,.\, \boldsymbol{\sigma}_i \,. \tag{1}$$

Here t (> 0) denotes the transfer integral of itinerant electrons between nearest-neighbour sites, ϵ_0 is the on-site potential of itinerant electrons, U is the on-site Coulomb repulsion between $\uparrow$ and $\downarrow$ spin itinerant electrons, $a^{\dagger}_{i\sigma}$ ($a_{i\sigma}$) is the creation (annihilation) operator of an itinerant electron at site i with σ, $n_{i\sigma} = a^{\dagger}_{i\sigma} a_{i\sigma}$, J (> 0) is the nearest-neighbour exchange interaction of local spins, K (> 0) represents the Hund couping, and $\boldsymbol{\sigma}_i$ stands for the Pauli matrix.

In the Schwinger boson technique (Read and Sachdev 1989; Arovas and Auerbach 1988; Auerbach and Arovas 1988; Hirsch and Tang 1989; Kane *et al.* 1990; Jayaprakash *et al.* 1989; Yoshioka 1989), the local spin can be expressed as $\mathbf{s} = \frac{1}{2} b^{\dagger}_{i\mu} \boldsymbol{\sigma}_i b_{i\nu}$ with a local constraint $\sum_{\mu} \langle b^{\dagger}_{i\mu} b_{i\mu} \rangle = 2S$ to ensure that the total number of bosons on each site is $2S$. Here S represents a local spin value. Then, the Hamiltonian becomes

$$H = -t \sum_{\langle ij \rangle \sigma} a^{\dagger}_{i\sigma} a_{j\sigma} + \sum_{i\sigma} \epsilon_0 a^{\dagger}_{i\sigma} a_{i\sigma} + \frac{U}{2} \sum_{i\sigma} n_{i\sigma} n_{i\bar{\sigma}}$$

$$+ J \sum_{\langle ij \rangle} b^{\dagger}_{i\alpha} b_{i\beta} b^{\dagger}_{j\gamma} b_{j\delta} (\sigma_{\alpha\beta} \sigma_{\gamma\delta} - \delta_{\alpha\beta} \delta_{\gamma\delta}) - \frac{K}{2} \sum_i \mathbf{S}_i \,.\, \boldsymbol{\sigma}_i \,. \tag{2}$$

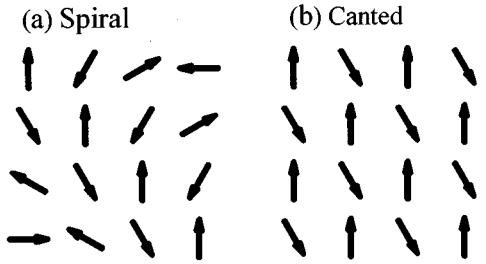

Fig. 1. Schematic illustrations of (a) a two-dimensional (1,1) SP state and (b) a CN state.

We consider the two dimensional (2d) case in this paper because the $Re_{1-x}A_xMnO_3$ system may be viewed as a quasi-2d one and its magnetic behaviour is mainly determined by the Mn–O plane. We introduce the spin order parameters $\langle \mathbf{S}_i \rangle$, $\langle \boldsymbol{\sigma}_i \rangle$, the resonating valence bond (RVB) order parameter $D_\eta = \langle b_{i\downarrow} b_{i+\eta\uparrow} - b_{i\uparrow} b_{i+\eta\downarrow} \rangle$, and the short-range ferromagnetic parameter $Q = \langle b^\dagger_{i\uparrow} b_{i+\eta\uparrow} + b^\dagger_{i\downarrow} b_{i+\eta\downarrow} \rangle$, where $\eta = x$ or y, and $i+x$ $(i+y)$ indicates a site next to the site i in the x (y) direction. Then, the Hamiltonian is decoupled. The Hund coupling here is assumed to be strong enough to make $\langle \boldsymbol{\sigma}_i \rangle$ approximately parallel to $\langle \mathbf{S}_i \rangle$. Illustrations for two-dimensional (1,1) SP and CN states are shown in Figs 1*a* and 1*b*, respectively. The relative angle between two spins on the two nearest-neighbour sites is $\theta_\eta = \theta_i - \theta_{i+\eta}$. We define $|\theta_\eta| = \pi + 2\theta$ with θ varing from 0 to $\pi/2$. By using a set of local spin quantisation axes, the mean field Hamiltonian is given by

$$
\begin{aligned}
H = & -t \sum_{\langle ij \rangle \sigma} \left[\cos\frac{\theta_\eta}{2} c^\dagger_{i\sigma} c_{j\sigma} + i \sin\frac{\theta_\eta}{2} c^\dagger_{i\sigma} c_{j\bar{\sigma}} \right] + \sum_{i\sigma} \upsilon_\sigma c^\dagger_{i\sigma} c_{i\sigma} \\
& + \frac{J}{6} \Bigg[\sum_{\langle ij \rangle} \Bigg[\left(Q_\eta \cos\frac{\theta_\eta}{2} \right) (g^\dagger_{j\uparrow} g_{i\uparrow} + g^\dagger_{j\downarrow} g_{i\downarrow}) - \left(i Q_\eta \sin\frac{\theta_\eta}{2} \right) (g^\dagger_{j\uparrow} g_{i\downarrow} + g^\dagger_{j\downarrow} g_{i\uparrow}) \\
& + \left(i D_\eta \sin\frac{\theta_\eta}{2} \right) (g^\dagger_{i\uparrow} g_{j\uparrow} - g^\dagger_{i\downarrow} g_{j\downarrow}) - \left(D_\eta \cos\frac{\theta_\eta}{2} \right) (g^\dagger_{i\uparrow} g^\dagger_{j\downarrow} - g^\dagger_{i\downarrow} g^\dagger_{j\uparrow}) \Bigg] + \text{h.c.} \Bigg] \\
& + \left(-\frac{4JS_d}{3} \cos 2\theta - \frac{K\sigma_s}{4} \right) \sum_{i\sigma} \sigma g^\dagger_{i\sigma} g_{i\sigma} \\
& - N \left(U n\uparrow n\downarrow + \frac{4JS_d^2}{3} \cos 2\theta + \frac{2J}{3} (|D|^2 - |Q|^2) + \frac{KS_d\sigma_s}{2} - 2S\lambda \right). \qquad (3)
\end{aligned}
$$

Here

$$
\begin{aligned}
\upsilon_\sigma &= \epsilon_0 + U n_{\overline{\sigma}} - \frac{\sigma K S_d}{2}, \\
Q_\eta &= \langle g^\dagger_{i\uparrow} g_{i+\eta\uparrow} + g^\dagger_{i\downarrow} g_{i+\eta\downarrow} \rangle \cos\frac{\theta_\eta}{2} + i \langle g^\dagger_{i\uparrow} g_{i+\eta\downarrow} + g^\dagger_{i\downarrow} g_{i+\eta\uparrow} \rangle \sin\frac{\theta_\eta}{2}, \\
D_\eta &= i \langle g_{i\uparrow} g_{i+\eta\uparrow} - g_{i\downarrow} g_{i+\eta\downarrow} \rangle \sin\frac{\theta_\eta}{2} + \langle g_{i\uparrow} g_{i+\eta\downarrow} - g_{i\downarrow} g_{i+\eta\uparrow} \rangle \cos\frac{\theta_\eta}{2}, \qquad (4)
\end{aligned}
$$

and N are the square lattice sites. In order to obtain the relation between $D_{-\eta}$ and D_η ($Q_{-\eta}$ and Q_η) for different states, it is convenient to consider the case of classical (large S) spins, in which $Q_\eta = \langle g^\dagger_{i\uparrow} g_{i+\eta\uparrow} \rangle \cos\frac{\theta_\eta}{2} = 2S e^{i\chi_{i+\eta} - \chi i} \cos\frac{\theta_\eta}{2}$, $D_\eta = i \langle g_{i\uparrow} g_{i+\eta\uparrow} \rangle \sin\frac{\theta_\eta}{2} = i 2S e^{i\chi_{i+\eta} + \chi i} \sin\frac{\theta_\eta}{2}$. We consider the case where D_η and Q_η are uniform. There is gauge freedom in choosing the phase χ_i, $\chi_{i+\eta}$ of D_η and Q_η. In the gauge $\chi_i = \chi_{i+\eta} = 0$, $D_\eta = -D_{-\eta} = D$, $Q_\eta = Q_{-\eta} = Q$ for the SP (1,1) state and $D_\eta = -D_{-\eta} = D$, $Q_\eta = -Q_{-\eta} = Q$ for the CN state.

For the SP state, the mean field Hamiltonian in momentum space is derived to be

$$H = H_s + H_d + E_0\,, \tag{5}$$

with

$$E_0 = N\Big[- Un\uparrow n\downarrow + \frac{4JS_d^2}{3}\cos 2\theta + \frac{KS_d\sigma_s}{2} + \frac{2J}{3}(|D|^2 - |Q|^2) - 2S\lambda\Big]\,. \tag{6}$$

Here H_s and H_d are itinerant electron and local spin parts, respectively, $S_d = |\langle \mathbf{S}_i\rangle|$, $\sigma_s = |\langle \sigma_i\rangle|$, and the Lagrange multiplier λ is introduced to enforce the condition $\sum_\mu \langle b_{i\mu}^\dagger b_{i\mu}\rangle = 2S$.

In equation (5), H_s and H_d are given as follows:

$$H_s = \sum_{\mathbf{k}} \epsilon BZ, \sigma[(v_\sigma - \epsilon_{\mathbf{k}}\sin\theta)c_{\mathbf{k}\sigma}^\dagger c_{\mathbf{k}}\sigma - \epsilon_{\mathbf{k}}^{'}\cos\theta c_{\mathbf{k}}^\dagger \sigma c_{k\sigma}]\,, \tag{7}$$

$$H_d = \sum_{\mathbf{k}\epsilon RBZ} \psi_{\mathbf{k}}^\dagger \tilde{H}_{\mathbf{k}} \psi'_{\mathbf{k}}\,. \tag{8}$$

with

$$\psi^\dagger = (g_{\mathbf{k}\uparrow}^\dagger - g_{-\mathbf{k}\downarrow} \quad g_{\mathbf{k}\downarrow}^\dagger \quad -g_{-\mathbf{k}\uparrow})\,,$$

$$\psi'^\dagger = (g_{\mathbf{k}\uparrow}^\dagger \quad g_{-\mathbf{k}\downarrow} \quad g_{\mathbf{k}\downarrow}^\dagger \quad g_{-\mathbf{k}\uparrow})\,,$$

$$\tilde{H} = \begin{pmatrix} j+\gamma & -d_2 & -q_2 & d_1 \\ d_2^* & j-\gamma & d_1^* & -q_2 \\ -q_2 & -d_1 & -j+\gamma & d_2 \\ -d_1^* & -q_2 & -d_2^* & -j-\gamma \end{pmatrix}.$$

Here the asterisk means congugate, k runs over the Brillouin zone (BZ) in H_s and half reduced Brillouin zone (RBZ) in H_d, and $\epsilon_{\mathbf{k}} = -2t(\cos k_x + \cos k_y)$, $\epsilon'_{\mathbf{k}} = -2t(\sin k_x + \sin k_y)$, $q_1 = -\frac{2J}{3}Q\sin\theta(\cos k_x + \cos k_y)$, $q_2 = \frac{2J}{3}Q\cos\theta(\sin k_x + \sin k_y)$, $d_1 = i\frac{2J}{3}D\cos\theta(\cos k_x + \cos k_y)$, $d_2 = -i\frac{2J}{3}\sin\theta(\sin k_x + \sin k_y)$, $j = \frac{4JS_d}{3}\cos\theta - \frac{K\sigma_s}{4}$, $\gamma = q_1 + \lambda - \frac{2J}{3}$. By a Bogoliubov transformation H_s diagonalises as

$$H_s = \sum_{\mathbf{k}\epsilon BZ,\sigma} [E_-^{SP}(\mathbf{k})d_{\mathbf{k}\uparrow}^\dagger d_{\mathbf{k}\uparrow} + E_+^{SP}(\mathbf{k})d_{\mathbf{k}\downarrow}^\dagger d_{\mathbf{k}\downarrow}]\,, \tag{9}$$

where

$$E_{\pm}^{SP}(\mathbf{k}) = v_0 - \epsilon_{\mathbf{k}}\sin\theta \pm (\Delta_E^2 + \epsilon_{\mathbf{k}}^{'2}\cos^2\theta)^{\frac{1}{2}}\,, \tag{10}$$

with $v_0 = (v_\downarrow + v_\uparrow)/2$ and $\Delta_E = (v_\downarrow - v_\uparrow)/2$. Here v_0 is the normalised on-site potential, and Δ_E is the effective field, which represents the strength of the Hund coupling. Since we assume that the Hund coupling is large, $\tilde{H}$ can be separated into two parts, namely $\tilde{H} = H_0 + H'$, with H' being the perturbation. Here H_0 and H' are given as follows:

$$H_0 = \begin{pmatrix} -\frac{K\sigma_s}{4} + \lambda_0 & & & \\ & -\frac{K\sigma_s}{4} - \lambda_0 & & \\ & & \frac{K\sigma_s}{4} + \lambda_0 & \\ & & & \frac{K\sigma_s}{4} - \lambda_0 \end{pmatrix},$$

$$H' = \begin{pmatrix} \tilde{\lambda} + q_1 & -d_2 & -q_2 & d_1 \\ d_2^* & -\tilde{\lambda} - \frac{8JS_d}{3}\cos2\theta + q_1 & d_1^* & -q_2 \\ -q_2 & -d_1 & \tilde{\lambda} + \frac{8JS_d}{3}\cos2\theta + q_1 & d_2 \\ -d_1^* & -q_2 & -d_2^* & -\tilde{\lambda} - q_1 \end{pmatrix}, \tag{11}$$

with $\tilde{\lambda} = \frac{4JS_d}{3}\cos2\theta + \lambda'$. In equation (11), the Lagrange multiplier λ has also been separated into two parts, namely $\lambda = \lambda_0 + \lambda'$. As an approximation, we take $\lambda_0 = K\sigma_s/4$ because $(\lambda_0 - K\sigma_s/4)$ is very small at low temperatures. Evaluating the eigenvalue of H_d to first order and the eigenfunction to zero order, we get

$$\begin{aligned} g_{\mathbf{k}\uparrow} &= \zeta_1 o_{\mathbf{k}\uparrow} + \zeta_2 o^\dagger_{-\mathbf{k}\uparrow}, \qquad g^\dagger_{-\mathbf{k}\downarrow} = o^\dagger_{-\mathbf{k}\downarrow}, \\ g_{\mathbf{k}\downarrow} &= o_{\mathbf{k}\downarrow}, \qquad g^\dagger_{-\mathbf{k}\uparrow} = \zeta_2 o_{\mathbf{k}\uparrow} + \zeta_1 o^\dagger_{-\mathbf{k}\uparrow}\,, \end{aligned} \tag{12}$$

with

$$\zeta_1 = \sqrt{\frac{\tilde{\lambda} + q_1}{2\omega_-^{SP}} + \tfrac{1}{2}}, \qquad \zeta_2 = \sqrt{\frac{\tilde{\lambda} + q_1}{2\omega_-^{SP}} - \tfrac{1}{2}},$$

$$\omega_-^{SP} = \sqrt{(\tilde{\lambda} + q_1)^2 - |d_1|^2}\,. \tag{13}$$

The approximate spinon energy spectra are

$$\omega_{-}^{SP} = \sqrt{(\tilde{\lambda}+q_1)^2 - |d_1|^2},$$

$$\omega_{+}^{SP} = \frac{8JS_d}{3}\cos 2\theta + \frac{K\sigma_s}{2} + \tilde{\lambda} + q_1\,. \tag{14}$$

The chemical potential of itinerant electron μ, the Lagrange multiplier $\tilde{\lambda}$, and the parameters σ_s, S_d, Q, D should be determined self-consistently as follows:

$$1 = \frac{1}{N}\sum_{\mathbf{k}\epsilon BZ}\left[\frac{1}{e^{\beta(E_{-}^{SP}-\mu)}+1} - \frac{1}{e^{\beta(E_{+}^{SP}-\mu)}+1}\right] \tag{15}$$

$$2S+\tfrac{1}{2} = \frac{1}{N}\sum_{\mathbf{k}\epsilon BZ}\left(\frac{\tilde{\lambda}+|q_1|}{2\omega_{-}^{SP}}\coth\frac{\beta\omega_{-}^{SP}}{2} + \frac{1}{\mathrm{e}^{\beta\omega_{+}^{SP}}-1}\right), \tag{16}$$

$$\sigma_s = \frac{1}{N}\sum_{\mathbf{k}\epsilon BZ}\sin(2\xi)\left[\frac{1}{\mathrm{e}^{\beta(E_{-}^{SP}-\mu)}+1} - \frac{1}{\mathrm{e}^{\beta(E_{+}^{SP}-\mu)}+1}\right], \tag{17}$$

$$S_d+\tfrac{1}{2} = \frac{1}{N}\sum_{\mathbf{k}\epsilon BZ}\left(\frac{\tilde{\lambda}+|q_1|}{2\omega_{-}^{SP}}\coth\frac{\beta\omega_{-}^{SP}}{2} - \frac{1}{\mathrm{e}^{\beta\omega_{+}^{SP}}-1}\right), \tag{18}$$

$$Q = \frac{\sin\theta}{N}\sum_{\mathbf{k}\epsilon BZ}\left(\frac{\tilde{\lambda}+|q_1|}{2\omega_{-}^{SP}}\coth\frac{\beta\omega_{-}^{SP}}{2} - \frac{1}{\mathrm{e}^{\beta\omega_{+}^{SP}}-1}\right), \tag{19}$$

$$D = \frac{JD}{2N}\cos^2\theta\sum_{\mathbf{k}\epsilon BZ}\frac{(\cos x+\cos y)^2}{2\omega_{-}^{SP}}\coth\frac{\beta\omega_{-}^{SP}}{2}\,, \tag{20}$$

with $\beta = 1/k_BT$, $\xi = \frac{1}{2}\arctan[\Delta_E/|\epsilon'_{\mathbf{k}}|\cos\theta]$.

For the CN state, we express $\sin(\theta_\eta/2)$ as a unified form, which is suitable to both sublattices A and B:

$$\sin(\theta_\eta/2) = \cos\theta\mathrm{e}^{\mathbf{i}\mathbf{k}_0\cdot\mathbf{R}_\mathrm{i}}\,, \tag{21}$$

with $\mathbf{k}_0 = (\pi,\pi)$. Then, the mean field Hamiltonian in momentum space becomes

$$H = H_s + H_d + E_0\,, \tag{22}$$

with

$$E_0 = N\left[-Un\uparrow n\downarrow + \frac{4JS_d^2}{3}\cos 2\theta + \frac{KS_d}{2} + \frac{2J}{3}(|D|^2-|Q|^2) - 2S\lambda\right]. \tag{23}$$

Here H_s and H_d are given as

$$H_s = \sum_{\mathbf{k}\epsilon BZ,\sigma} [(v_\sigma - \epsilon_{\mathbf{k}} \mathrm{sin}\theta) c^\dagger_{\mathbf{k}\sigma} c_{\mathbf{k}\sigma} + i\epsilon_{\mathbf{k}} \mathrm{cos}\theta c^\dagger_{\mathbf{k}\sigma} c_{\overline{\mathbf{k}\sigma}}] \,, \tag{24}$$

$$H_d = \sum_{\mathbf{k}\epsilon RBZ} \psi^\dagger_{\mathbf{k}} \tilde{H}_{\mathbf{k}} \psi'_{\mathbf{k}} \,, \tag{25}$$

with

$$\psi^\dagger = (g^\dagger_{\mathbf{k}\uparrow} \quad -g_{-\mathbf{k}\downarrow} \quad g^\dagger_{\tilde{\mathbf{k}}\downarrow} \quad -g_{-\tilde{\mathbf{k}}\uparrow}), \qquad \psi'^\dagger = (g^\dagger_{\mathbf{k}\uparrow} \quad -g_{-\mathbf{k}\downarrow} \quad g^\dagger_{\tilde{\mathbf{k}}\downarrow} \quad -g_{-\tilde{\mathbf{k}}\uparrow}),$$

$$\tilde{H} = \begin{pmatrix} j+\gamma & d_3 & -q_4 & d_4 \\ -d_3^* & j_2-\gamma & -d_4^* & q_4 \\ -q_4^* & d_4 & -j+\gamma & d_3 \\ -d_4^* & q_2^* & -d_3^* & -j-\gamma \end{pmatrix} , \tag{26}$$

where $\epsilon_{\mathbf{k}} = -2t(\mathrm{cos}k_x + \mathrm{cos}k_y)$, $\tilde{\mathbf{k}}$ is the reduced wave-vector of $\mathbf{k}+\mathbf{k}_0$, $q_3 = i\frac{2J}{3}Q\mathrm{sin}\theta(\mathrm{sin}k_x+\mathrm{sin}k_y)$, $q_4 = \frac{2J}{3}Q\mathrm{cos}\theta(\mathrm{sin}k_x+\mathrm{sin}k_y)$, $d_3 = i\frac{2J}{3}D\mathrm{sin}\theta(\mathrm{sin}k_x+\mathrm{sin}k_y)$, $d_4 = i\frac{2J}{3}\mathrm{cos}\theta(\mathrm{sin}k_x + \mathrm{sin}k_y)$, $j = -4JS\mathrm{cos}2\theta/3 - K\sigma_s/4 + q_3$, $\gamma = \lambda - 2J/3$. By using a Bogoliubov transformation, we obtain the energy spectra for an itinerant electron,

$$E^{CN}_{\pm}(\mathbf{k}) = v_o \pm (\Delta^2_E + \epsilon^2_{\mathbf{k}} \pm 2\Delta_E \epsilon_{\mathbf{k}} \mathrm{sin}\theta)^{\frac{1}{2}} \,. \tag{27}$$

Using a similar procedure to simplify the spinon part in the SP state, we get

$$\begin{aligned} g_{\mathbf{k}\uparrow} &= \zeta_1 \sigma_{\mathbf{k}\uparrow} + \zeta_2 o^\dagger_{-\tilde{\mathbf{k}}\uparrow}, \qquad g^\dagger_{-\mathbf{k}\downarrow} = o^\dagger_{-\mathbf{k}\downarrow}, \\ g_{\tilde{\mathbf{k}}\downarrow} &= o_{\tilde{\mathbf{k}}\downarrow}, \qquad g^\dagger_{-\tilde{\mathbf{k}}\uparrow} = \zeta_2 o_{\mathbf{k}\uparrow} + \zeta_1 o^\dagger_{-\tilde{\mathbf{k}}\uparrow} \,, \end{aligned} \tag{28}$$

with

$$\zeta_1 = \sqrt{\frac{\tilde{\lambda}+q_3}{2\omega^{CN}_-} + \tfrac{1}{2}}, \qquad \zeta_2 = \sqrt{\frac{\tilde{\lambda}+q_3}{2\omega^{CN}_-} - \tfrac{1}{2}},$$

$$\omega^{CN}_- = \sqrt{(\tilde{\lambda}+q_3)^2 - |d_4|^2} \,. \tag{29}$$

The approximate spinon energy spectra are

$$\omega^{CN}_- = \sqrt{(\tilde{\lambda}+q_3)^2 - |d_4|^2} \,,$$

$$\omega^{CN}_+ = \frac{8JS_d}{3}\mathrm{cos}2\theta + \frac{K\sigma_s}{2} + \tilde{\lambda} + q_3 \,. \tag{30}$$

The self-consistent equations to determine the itinerant electron potential μ, the Lagrange multiplier $\tilde{\lambda}$, and the parameters for the CN state are

$$1 = \frac{1}{N}\sum_{\mathbf{k}\epsilon BZ}\left(\frac{1}{\mathrm{e}^{\beta(E_-^{CN}-\mu)}+1} - \frac{1}{\mathrm{e}^{\beta(E_+^{CN}-\mu)}+1}\right), \tag{31}$$

$$2S+\tfrac{1}{2} = \frac{1}{N}\sum_{\mathbf{k}\epsilon BZ}\left(\frac{\tilde{\lambda}+|q_1|}{2\omega_-^{CN}}\mathrm{coth}\frac{\beta\omega_-^{CN}}{2} + \frac{1}{\mathrm{e}^{\beta\omega_+^{CN}}-1}\right), \tag{32}$$

$$\sigma_s = \frac{1}{N}\sum_{\mathbf{k}\epsilon BZ}\sin(2\chi)\left[\frac{1}{\mathrm{e}^{\beta(E_-^{CN}-\mu)}+1} - \frac{1}{\mathrm{e}^{\beta(E_+^{CN}-\mu)}+1}\right], \tag{33}$$

$$S_d+\tfrac{1}{2} = \frac{1}{N}\sum_{\mathbf{k}\epsilon BZ}\left(\frac{\tilde{\lambda}+|q_1|}{2\omega_-^{CN}}\mathrm{coth}\frac{\beta\omega_-^{CN}}{2} - \frac{1}{\mathrm{e}^{\beta\omega_+^{CN}}-1}\right), \tag{34}$$

$$Q = \frac{\sin\theta}{N}\sum_{\mathbf{k}\epsilon BZ}\left(\frac{\tilde{\lambda}+|q_1|}{2\omega_-^{CN}}\mathrm{coth}\frac{\beta\omega_-^{CN}}{2} - \frac{1}{\mathrm{e}^{\beta\omega_+^{CN}}-1}\right), \tag{35}$$

$$D = \frac{JD}{2N}\cos^2\theta\sum_{\mathbf{k}\epsilon BZ}\frac{(\mathrm{cos}x+\mathrm{cos}y)^2}{2\omega_-^{CN}}\mathrm{coth}\frac{\beta\omega_-^{CN}}{2}, \tag{36}$$

with $\beta = 1/k_BT$ and $\chi = \frac{1}{2}\mathrm{arctan}[(\Delta_E - \epsilon_{\mathbf{k}}\mathrm{sin}\theta)/|\epsilon_{\mathbf{k}}|\mathrm{cos}\theta]$.

In order to determine θ, the free energy should be calculated. The calculated free energy per site is given as

$$\begin{aligned} f = & -\frac{k_BT}{N}\sum_{\mathbf{k}\epsilon BZ}[\ln(1+\mathrm{e}^{-\beta(E_--\mu)}) + \ln(1+\mathrm{e}^{-\beta(E_+-\mu)})] \\ & + \frac{k_BT}{N}\sum_{\mathbf{k}\epsilon BZ}[\ln(1-\mathrm{e}^{-\beta\omega-}) + \ln(1-\mathrm{e}^{-\beta\omega+})] \\ & - \frac{2J}{3}(|D|^2-|Q|^2) - \frac{4JS_d^2}{3}\cos2\theta + \mu(1-x)\,. \end{aligned} \tag{37}$$

For the SP state, we have $E_\pm = E_\pm^{SP}$, $\omega_\pm = \omega_\pm^{SP}$, while for the CN state, $E_\pm = E_\pm^{CN}$, $\omega_\pm = \omega_\pm^{CN}$. By minimising the free energy, we calculate the phase diagram. We take $t = 1$ for convenience. We select $\Delta'_E = KS/2 = 5$, which

corresponds to a large Hund coupling (Inoue *et al.* 1995) and $JS^2 = 0{\cdot}01$ such that an FM phase appears in an intermediate x region at $T = 0$ (Jiang *et al.* 1997). The detailed calculation process is as follows. First, given values of x and $k_B T$, we calculate μ, $\tilde{\lambda}$, σ_s, S_d, Q, D self-consistently through equations (15)–(20) [or equations (31)–(36)] with θ varying from 0 to $\pi/2$. Then, we substitute the values obtained into equation (37) and get a series of free energies for the SP (or CN) state. Comparing the free energies with respect to θ, we get a minimal free energy $F_{\min}(\theta)$. If the θ corresponding to $F_{\min}(\theta)$ is 0, the system is in AF; if it is $\pi/2$, the system is in FM; if it is not 0 and $\pi/2$, the system is in the SP or CN state. Finally, let x vary from 0 to 1 and $k_B T$ vary from 0 to a finite value, then we get the phase diagram in the $x - k_B T$ plane.

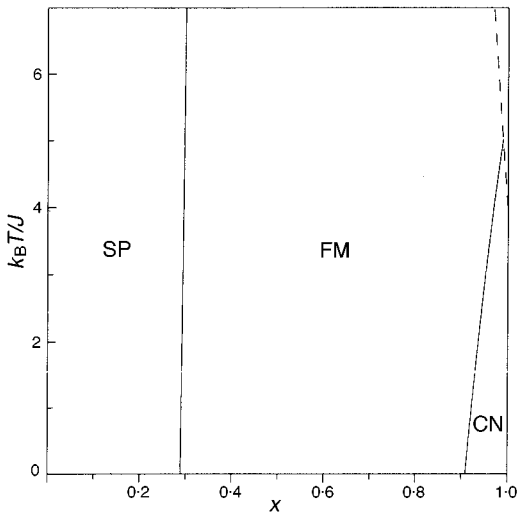

Fig. 2. Magnetic phase diagrams in the $x - k_B T$ plane with $\Delta'_E = 5$ and $JS^2 = 0{\cdot}01$. The area enclosed by the dashed line and the line $x = 1$ is the region of the PM state.

3. Results and Discussion

The phase diagram is shown in Fig. 2, from which we can see that when $T \to 0$ the system is in the AF state at $x = 0$ and $x = 1$, and in a SP state in the lower x region. Then it changes into the FM state in an intermediate x region and finally is in a CN state in the higher x region. A PM phase appears near $x \sim 1$ with T increasing to a certain value. Fig 3*a* and 3*b* show parameters Q and D respectively. In the FM state Q reaches its maximum value and $D = 0$. In the PM state $Q = 0$, $D = 0$. When $T \to 0$, $Q = 0$ and D reaches its maximum value at $x = 0$ and 1. Both Q and D decrease with T increasing. When T reaches a certain value T_Q, Q disappears and when T reaches a certain value T_D, D disappears. The critical temperatures T_D and T_Q vary with the doping concentration x.

Now we calculate the spin–spin correlation function:

$$\langle \mathbf{S}_0 \,.\, \mathbf{S}_i \rangle = \frac{\cos\theta_i}{4N^2} \sum_{\mathbf{k},\mathbf{k}'\epsilon BZ} \cos\mathbf{k}\mathbf{r}_i \, \cos\mathbf{k}'\mathbf{r}_i$$

$$\times \left[\frac{d^*(\mathbf{k})}{2\omega_-(\mathbf{k})} \cos\frac{\beta\omega(\mathbf{k})}{2} \frac{d(\mathbf{k}')}{2\omega_-(\mathbf{k}')} \coth\frac{\beta\omega(\mathbf{k})}{2} \right.$$

$$\times \frac{\tilde{\lambda} + q(\mathbf{k})}{2\omega_-^{SP}(\mathbf{k})} \coth\frac{\beta\omega_-(\mathbf{k})}{2} \frac{\tilde{\lambda} + q(\mathbf{k}')}{2\omega_-(\mathbf{k}')} \coth\frac{\beta\omega_-(\mathbf{k}')}{2}$$

$$\left. + \frac{\mathrm{e}^{\beta\omega-(\mathbf{k})} + \mathrm{e}^{\beta\omega+(\mathbf{k}')}}{(\mathrm{e}^{\beta\omega+(k')} - 1)(\mathrm{e}^{\beta\omega-(\mathbf{k}')} - 1)} + \frac{\mathrm{e}^{\beta\omega+(\mathbf{k})}}{(\mathrm{e}^{\beta\omega+(\mathbf{k}')} - 1)^2} \right]$$

$$+ \frac{1}{4N^2} \sum_{\mathbf{k},\mathbf{k}'\epsilon BZ} \cos\mathbf{k}\mathbf{r}_i \, \cos\mathbf{k}'\mathbf{r}_i \frac{\mathrm{e}^{\beta\omega-(\mathbf{k})} + \mathrm{e}^{\beta\omega+(\mathbf{k}')}}{(\mathrm{e}^{\beta\omega-(\mathbf{k})} - 1)(\mathrm{e}^{\beta\omega+(\mathbf{k}')} - 1)} \,. \quad (38)$$

For the SP state, $d(\mathbf{k}) = i2J/3D\cos\theta(\cos k_x + \cos k_y)$ and $q(\mathbf{k}) = -2J/3Q\sin\theta(\cos k_x + \cos k_y)$. For the CN state, $d(\mathbf{k}) = i2J/3\cos\theta(\sin k_x + \sin k_y)$ and $q(\mathbf{k}) = i2J/3Q\sin\theta(\sin k_x + \sin k_y)$. In the case that $T = 0$ and $|\mathbf{r}_i| \to \infty$, the spin–spin correlation function is given by $\langle \mathbf{S}_0 \,.\, \mathbf{S}_i \rangle = \frac{\cos\theta_i}{4} \frac{n_0^2}{N^2}$ which represents long range spin correlation at $T = 0$ due to the spinon's Bose condensation. At finite temperatures, there is no Bose condensation for the exact 2d situation and so the correlation decays exponentially. Therefore, there is no long range order (LRO). The spin–spin correlation between two spins on the two nearest-neighbour sites is $\langle \mathbf{S}_0 \,.\, \mathbf{S}_\eta \rangle \sim (Q^2 - D^2)$, which indicates that Q promotes short range ferromagnetic correlation and D short range antiferromagnetic correlation. Because $Q \neq 0$ for $T < T_Q$ and $D \neq 0$ for $T < T_D$, a short range spin correlation exists as long as T is lower than the largest temperature between T_Q and T_D.

In order to obtain the phase diagram we minimise the system's free energy with respect to θ, which characterises the relative angle between two spins on the two nearest-neighbour sites. Because LRO does not exist the AF, SP, FM and CN states obtained actually represent AF, SP, FM and CN short range correlation with finite correlation length, respectively. For convenience, we still call them AF, SP, FM and CN states. With T increasing, the correlation length decreases. When T is higher than the largest temperature between T_Q and T_D, the correlation length decreases to zero, all short range correlation disappears, and the system is in a PM state. On the other hand, the $\mathrm{Re}_{1-x}\mathrm{A}_x\mathrm{MnO}_3$ system may be viewed as a quasi-2d one, where LRO can be sustained. Therefore, the present so-called AF, SP, FM and CN states with short range correlation correspond to the $\mathrm{Re}_{1-x}\mathrm{A}_x\mathrm{MnO}_3$ system AF, SP, FM and CN states with LRO respectively.

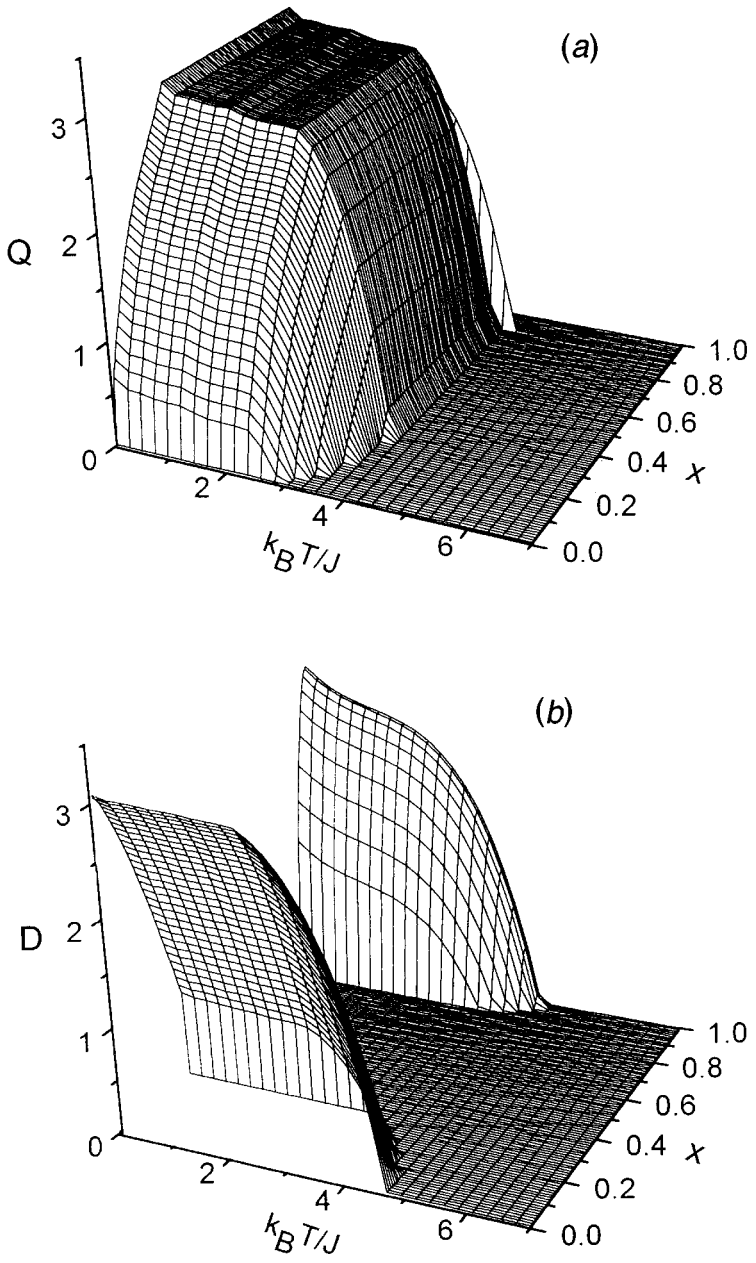

Fig. 3. (a) The short-range ferromagnetic parameter Q. (b) The RVB order parameter D.

4. Conclusion

In summary, using the Schwinger boson method we get a detailed phase diagram of Mn oxides at low temperatures based on an electron–electron correlation mechanism. Our results show that a PM state may first appear in the higher

doping concentrations with T increasing. We also obtain a spin–spin correlation which has not been obtained before in the ordinary mean field treatment.

Acknowledgments

This work was supported by a Chinese Natural Science Foundation Grant No. 19677202.

References

Anderson, P. W., and Hasegawa, H. (1955). *Phys. Rev.* **100**, 675.
Arovas, D. P., and Auerbach, A. (1988). *Phys. Rev.* B **38**, 316.
Auerbach, A., and Aovas, D. P. (1988). *Phys. Rev. Lett.* **61**, 617.
Hirsch, J. E., and Tang, S. (1989). *Phys. Rev.* B **39**, 2850.
Hwang, H. Y., Cheong, S. W., Radaelli, P. G., Marezio, M., and Batlogg, B. (1995). *Phys. Rev. Lett.* **75**, 914.
Ibarra, M. R., *et al.* (1995). *Phys. Rev. Lett.* **75**, 3541.
Inoue, J., and Maekawa, S. (1995). *Phys. Rev. Lett.* **74**, 3407.
Jayaprakash, C., Krishnamurthy, H. R., and Sarker, S. (1989). *Phys. Rev.* B **40**, 2610.
Jiang, J., Dong, J., and Xing, D. Y. (1997). *Phys. Rev.* B **55**, 8973.
Ju, H. L., Kwon, C., Li, Q., Greene, R. L., and Venkatesan, T. (1994). *Appl. Phys. Lett.* **65**, 2108.
Kane, C. L., Lee, P. A., Ng, T. K., Chakraborty, B., and Read, N. (1990). *Phy. Rev.* B **41**, 2653.
Mills, A. J., Littlewood, P. B., and Shraiman, B. I. (1995). *Phys. Rev. Lett.* **74**, 5144.
Mills, A. J., Shraiman, B. I., and Mueller, R. (1996). *Phys. Rev. Lett.* **77**, 175.
Read, N., and Sachdev, S. (1989). *Phys. Rev. Lett.* **62**, 1694.
von Helmolt, R., *et al.* (1993). *Phys. Rev. Lett.* **71**, 2331.
von Helmolt, R., *et al.* (1994). *J. Appl. Phys.* **76**, 6925.
Yoshioka, D. (1989). *J. Phys. Soc. Jpn* **58**, 3733.
Zener, C. (1951). *Phys. Rev.* **81**, 440; **82**, 403.

Manuscript received 9 October 1996, accepted 12 May 1997